[American Journal of Science, Vol. 309, November, 2009, P. 775–787, DOI 10.2475/09.2009.01]

QUANTITATIVE UNCERTAINTY ANALYSES OF ANCIENT ATMOSPHERIC CO_2 ESTIMATES FROM FOSSIL LEAVES

DAVID J. BEERLING*†, ANDREW FOX*, and CLIVE W. ANDERSON**

ABSTRACT. The relationship between atmospheric CO_2 and ancient climate is of fundamental importance for gauging the climate sensitivity of the Earth system to a changing CO_2 regime. One of the most widely adopted paleobiological CO_2 proxies for reconstructing Earth's atmospheric CO_2 history exploits the inverse relationship between leaf stomatal index, the fraction of leaf epidermal cells that are stomatal structures, and atmospheric CO_2. However, fossil leaf-based CO_2 reconstructions make *a priori* assumptions about the form of the empirical relationship between SI and CO_2 required for transfer functions and have failed to correctly propagate error terms. These effects can translate into erroneous interpretations that undermine the value of the proxy. Here we report the development and application of a rigorous generalized statistical framework overcoming these limitations that generates probability density functions for each atmospheric CO_2 estimate. The utility of our statistical tools is demonstrated by showing how they revise earlier atmospheric CO_2 estimates from fossil cuticles of *Ginkgo* and *Metasequoia* trees during the early Eocene and middle Miocene warm periods upwards by +150 to 250 ppm to 450 to 700 ppm. The revised CO_2 reconstructions therefore help to resolve the paradox of warm Paleogene and Neogene "greenhouse" climates co-existing with near present-day levels of CO_2 and support the emerging view from independent paleoclimate studies for a high climate sensitivity of the Earth system. The statistical tools presented are sufficiently versatile to permit their use in other investigations of paleoCO_2 estimates from fossil leaves.

INTRODUCTION

Stomatal index (SI, percentage of leaf epidermal cells that are stomata) influences the gas exchange capacity of leaves by controlling the supply of CO_2 into the leaf for photosynthesis and the loss of water vapor. Experimental analyses indicate SI is under genetic control (Gray and others, 2000; Bergmann and others, 2004) and regulated by long distance CO_2 signalling between different parts of the plant (Lake and others, 2001). The non-linear inverse relationship between SI and atmospheric CO_2 during leaf development seen in experimental systems permits SI values determined from fossil leaf cuticles to be adopted as a terrestrial CO_2 proxy complementary to other paleobiological and geochemical CO_2 indicators (Royer and others, 2001a; Beerling and Royer, 2002a, 2002b). Notably, all of the biological and geochemical paleo-CO_2 proxies included in the IPCC (2007) report involve regression transfer functions to calibrate measurements on fossilized materials and require mathematical models to translate this quantity into an estimate of atmospheric CO_2 concentration. The input parameters to these models are also often known only imprecisely. However, few studies have addressed quantification of these different sources of uncertainties within a formal statistical framework allowing correct propagation of error terms (Freeman and Pagani, 2005; Fletcher and others, 2008). Consequently, the limitations of estimated atmospheric CO_2 values from proxies continue to remain a significant issue that must be addressed if we are to move towards a consensus on Earth's CO_2 history, and better constrain our understanding of its climate sensitivity (Royer, 2006; Hansen and others, 2008).

* Department of Animal and Plant Sciences, University of Sheffield, Sheffield S10 2TN, United Kingdom
** Department of Probability and Statistics, University of Sheffield, Sheffield S10 2TN, United Kingdom
† Corresponding author: d.j.beerling@sheffield.ac.uk

Here, we report the development and application of an alternative statistical framework overcoming two significant issues associated with obtaining reliable quantitative estimates of ancient atmospheric CO_2 concentrations using fossil leaf cuticles: (1) the need to make major *a priori* assumptions about the form of the SI-CO_2 response and (2) problematic (that is, incorrect) propagation of error terms in measurements of SI and CO_2 (Van der Burgh and others, 1993; Kürschner and others, 1997, 2008; Wagner and others, 1999; Retallack, 2001, 2002; Royer and others, 2001b; Royer, 2003; McElwain, 2004). Furthermore, the resulting functions are not always consistent with expectations based on diffusion theory of CO_2 through stomatal pores (Wynn, 2003; Konrad and others, 2008). We directly address these limitations by describing the decrease in SI with increasing CO_2 using non-parametric smooth monotonic curves (Ramsey and Silverman, 2002), and adopt direct simulation methods to integrate the different sources of uncertainty. A key output is the generation of probability density functions (PDFs) for each CO_2 estimate that can be analyzed for classical statistical descriptors. The approach builds on, and extends, earlier statistical work aimed at developing reliable age-depth relationships in Quaternary lacustrine sediments with overlapping probability distributions of ^{14}C dates (Enters and others, 2006).

We evaluated the utility of the statistical tools by computing new SI-CO_2 transfer functions for two detailed training datasets of SI measurements on *Ginkgo biloba* and *Metasequoia glyptostroboides* leaves taken from herbarium sheets dating back over the last 145 yr, and from saplings grown in greenhouses at four discrete CO_2 concentrations (Royer and others, 2001b; Royer, 2003). Revised atmospheric CO_2 estimates from fossil leaf cuticle SI measurements dating to the Paleogene and Neogene are then computed using these new functions for comparison with previous values (Royer and others, 2001b; Retallack, 2002; Royer, 2003) that suggested warm climates with comparatively low atmospheric CO_2 concentrations. Our statistical technique is flexible, being able to readily accommodate variable numbers of SI-CO_2 pairs of points in the training set, and therefore suitable for use in future investigations of CO_2 from fossil leaves.

MATERIALS AND METHODS

Construction of SI-CO_2 Transfer Function

We first addressed the issue of uncertainty in measurements of SI and CO_2 through a simulation approach whereby 2000 member random samples are generated for each data point in the training datasets for *Ginkgo* and *Metasequoia* (Royer and others, 2001b; Royer, 2003). These samples were generated using the mean and standard error of the SI measurements, and estimated uncertainty in the CO_2 concentrations from atmospheric flask data (http://cdiac.esd.ornl.gov/trends/co2/sio-keel-flask/sio-keel-flask.html) and CO_2 logging records from experiments (Beerling and Osborne, 2002), assuming independent Gaussian error distributions. This procedure allowed us to generate 2000 new training pseudo-datasets representing the range of possible SI-CO_2 combinations consistent with observations.

In the next step, curves were fitted to each pseudo-training dataset using monotone smoothing functions (Ramsay, 1998; Ramsay and Silverman, 2002; Enters and others, 2006). The approach rests on the fact that any twice differentiable strictly monotonic function, $S(c)$ say, of CO_2 concentration c may be expressed as

$$S(c) = a + b \int_0^c \exp\left(\int_0^u z(v)dv \right) du \qquad (1)$$

where a and b are constants and z is an unconstrained function, the relative acceleration of S with respect to c: $z(c) = S''(c)/S'(c)$. We estimated the curve S by estimating the

function z using 6th order B-splines, a set of polynomials of degree 5 joined end-to-end at knots (here taken as the data points) and with continuous derivatives up to order 4 across the c-domain. The fitting is based on the minimization of a penalized least squares criterion in which the discrepancy between $S(c)$ and observations (measured by squared differences) is augmented by a roughness penalty of the form

$$\lambda \int [z''(v)]^2 dv \tag{2}$$

where λ is a positive parameter. Roughness is thus measured by the integrated square of the second derivative of z. The order of the B-spline basis for z was chosen to ensure adequate smoothness of z''; a 6th order basis, which guarantees continuous slope and curvature (first and second derivatives) for z', proved acceptable. The parameter λ governs the compromise between the smoothness of the curve and how closely it passes to data points. A zero λ, for example, will yield a monotonic curve $S(c)$ passing as close to individual data points as possible, but possibly with unrealistic plateaus and very steep intervals; on the other hand, as λ becomes very large the curve will approximate one whose relative acceleration function $z(c) = S''(c)/S'(c)$ is linear, over-summarizing the structure in the data.

We chose λ with the following 12-fold cross-validation procedure. Each complete training dataset was divided into 12 approximately equal parts; then for a specified value of λ the procedure described above was used to estimate a curve $S(c)$ on the basis of 11 of the parts, and the result was compared to the data from the remaining part by calculating the value of the penalized least squares function. This procedure was repeated for all twelve parts and the resulting penalized functions were averaged. The same calculations were carried out for a range of λ values. We sought a single value of λ generally yielding low values of the penalized functions and found that $\lambda = 100$ met this requirement.

Reconstruction of Atmospheric CO_2 Estimate from Fossil SI Measurements

To estimate CO_2 from fossil SI observations, 500 estimates of fossil cuticle SI values were simulated from the mean and standard errors of each measurement, assuming Gaussian error distributions. Atmospheric CO_2 values corresponding to these 500 SI values (rounded to 3 decimal places) were then derived by inversion from each of the 2000 fitted curves. A kernel density estimate of the PDF of these CO_2 values for each fossil SI observation was then constructed (Silverman, 1986). Corresponding 95 percent confidence intervals for CO_2 were estimated from the 2.5 and 97.5 percentiles of the inverted values.

All coding was undertaken with the MATLAB® software package, and annotated versions of the code (STOM_CO2_STATS) are archived in the free software library of the World Data Centre for Paleoclimatology, NOAA (http://www.ncdc.noaa.gov/paleo/softlib/softlib.html).

RESULTS AND DISCUSSION

The resulting SI-CO_2 relationships, expressed by the point-wise median and 2.5 and 97.5 percentiles of the 2000 response functions, accurately capture observations for both *Ginkgo* and *Metasequoia* (fig. 1). The fitted monotonic spline functions for both species are very similar to the empirical functions selected by Royer and others (2001b) and Royer (2003) at CO_2 concentrations < 350 ppm, but diverge at higher CO_2 concentrations. Although considerably less subjective than the *a priori* selection of particular functions describing the changes in SI with CO_2, it is important to recognize that an element of subjectivity remains in the choice of the smoothing parameter λ,

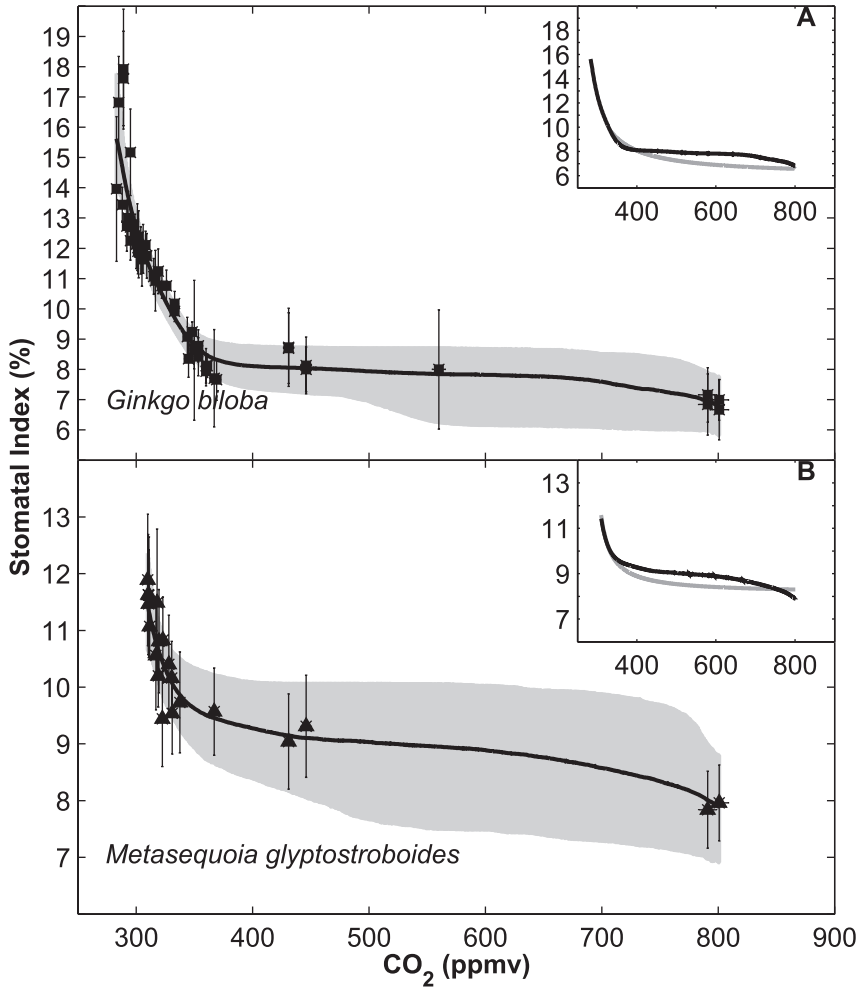

Fig. 1. Non-linear functions describing the response leaf stomatal index (SI, ± 1 std. dev.) atmospheric CO_2 (mean ± 1 std. dev.) for (A) *Ginkgo* and (B) *Metasequoia*. The curves shown are the median (solid line), the shaded areas for each one represents the 95% confidence intervals generated after incorporating SI and CO_2 errors, assuming Gaussian distributions and fitting 2000 monotone smoothing functions (see text for details). Insets show the new functions (bold line) and those reported by Royer and others (2001b) (gray line).

and the placement of knots. Moreover the choice of the class of functions fitted rests on the assumption that the underlying relationship between SI and CO_2 is monotonic decreasing. Significantly, however, the new functions reveal more accurately the "actual" envelope of uncertainty obtained after propagating uncertainties associated with (i) training dataset measurements, (ii) curve fitting procedures, and (iii) fossil leaf observations, through the inversion process, rather than obtained simply by calculating confidence limits from dispersion statistics of mean SI values.

Our functions strengthen the basis for translating fossil SI measurements into PDFs of atmospheric CO_2. The shape of the atmospheric CO_2 PDFs predicted from leaf SI values reflects the non-linear nature of the SI-CO_2 responses, with increasing uncertainty at higher CO_2 levels, as illustrated by a suite of examples depicted in

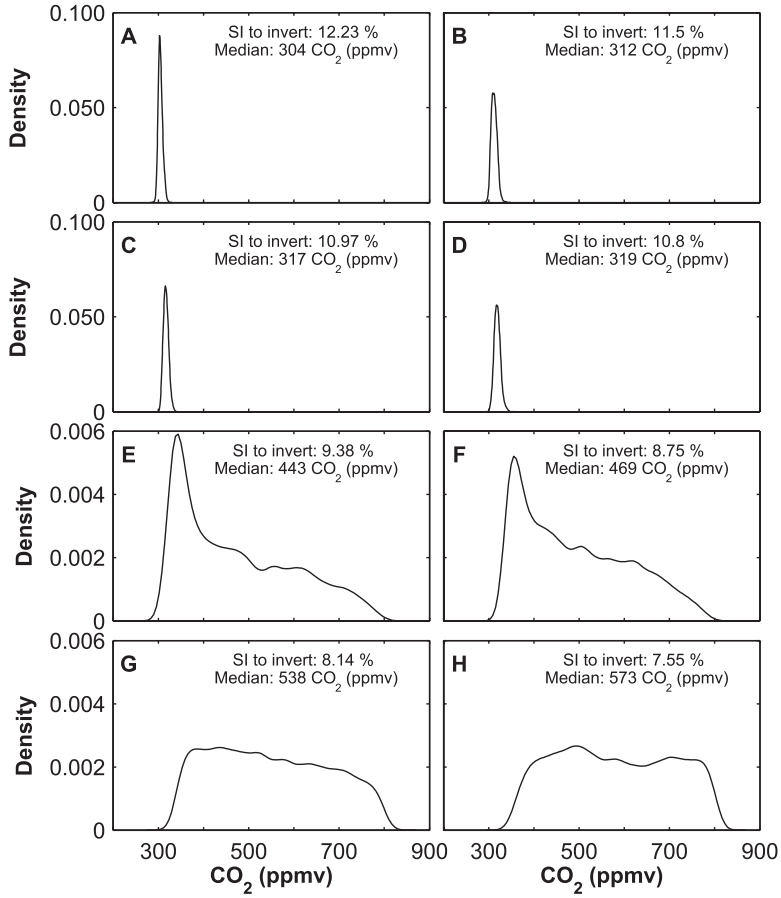

Fig. 2. Selected probability density functions for ancient atmospheric CO_2 predictions based on actual fossil leaf *Ginkgo* stomatal index (SI) measurements from Royer and others (2001b).

figure 2. This generally neglected effect of increased uncertainty at high CO_2, as opposed to decreased sensitivity which is often noted (Royer and others, 2001a), is a characteristic of all CO_2 proxies resting on non-linear calibration functions, including alkenones (Freeman and Pagani, 2005; Pagani and others, 2005; Henderiks and Pagani, 2007) and boron isotopes (Demicco and others, 2003). When fossil SI values are relatively high, the CO_2 PDF is tightly constrained (figs. 2 A-D), but as they decrease the uncertainty in inverted atmospheric CO_2 estimates rises, as reflected by the increased dispersion of the PDFs (figs. 2 E-H). For *Ginkgo,* SI values between ca. 8 to 9 percent, lead to skewed CO_2 PDFs (figs. 2, E, F), and at even lower values still (7-8%) the PDFs have broad distributions encompassing nearly the whole range of the training dataset CO_2. It is important to recognize that this shift in the form of the PDF reflects the greater variation in curve fitting possibilities at low SI-high CO_2 as the response becomes asymptotic, rather than increased measurement uncertainty (fig. 1).

Nevertheless, the widest 95 percent confidence limits for *Ginkgo* with SI values of 7 to 8 are calculated to be on the order of ± 200 ppm, larger than those of the alkenone proxy (40-56 ppm) (Pagani and others, 2005; Henderiks and Pagani, 2007), but better

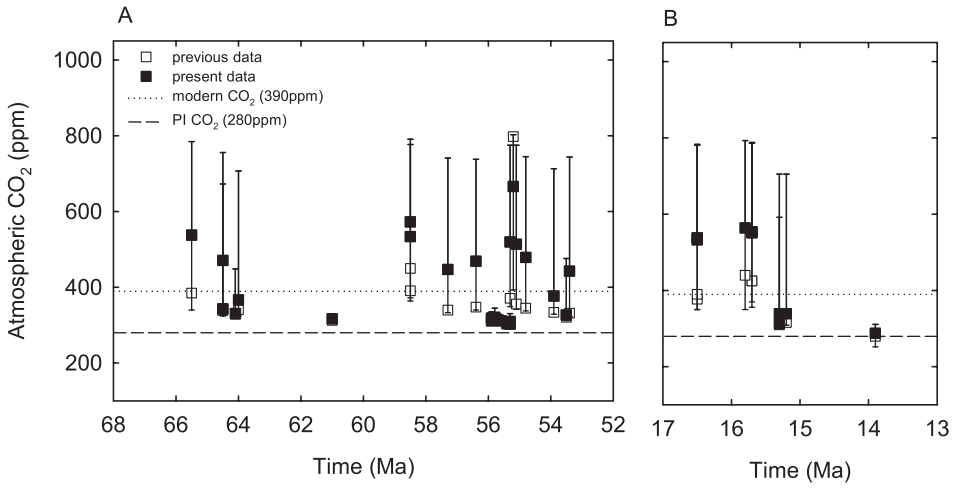

Fig. 3. Reconstructed atmospheric CO_2 concentrations during (A) the Paleogene and (B) the Neogene. Solid symbols show revised CO_2 reconstructions ("present data"), open symbols show "previous data" reported by Royer and others (2001b) and Retallack (2002). Present data display median values ± 95% confidence (table 1). PI = pre-industrial.

than other CO_2 proxies. Error terms of the boron isotope method, for example, are around 1500 ppmv (Demicco and others, 2003), and for paleosols over 1000 ppm (Ekart and others, 1999; Breecker and others, 2009) for the Paleogene. However, more reliable constraints on the errors of these proxies require quantitative uncertainty analyses, including robust propagation of error terms in the measurements and model functions used to convert them into CO_2 values.

Application of the new statistical transfer functions to estimate atmospheric CO_2 values and 95 percent confidence limits from SI measurements on fossil Paleogene and Neogene *Ginkgo* and *Metasequoia* cuticles (Royer and others, 2001b; Retallack, 2002; Royer, 2003) yield estimates higher in 86 percent of cases than before using the same training datasets (fig. 3; table 1). Stomatal-based Cenozoic atmospheric CO_2 estimates all exceed the pre-industrial concentration, with most exceeding the present-day value (fig. 3). During the Paleogene (58-54 Ma), median reconstructed atmospheric CO_2 levels are typically 450 to 700 ppm, compared to 300 to 400 ppm reported previously (fig. 3A). Upwards revision of these numbers closes the gap with revised boron isotope estimates that reveal CO_2 concentrations decline from ca. 1500 to 700 ppm between 60 and 52 Ma (Demicco and others, 2003). Further rapprochement between the approaches might be possible after accounting for the uncertainties between the two datasets. During the Neogene (18-14 Ma), including the middle Miocene climatic optimum, we obtain peak CO_2 concentrations of 500 to 600 ppm, compared to 300 to 400 ppm reported previously from stomata (fig. 3B). These numbers exceed values from some (Pagani and others, 2005) but not all alkenones (Freeman and Hayes, 1992; Stott, 1992), and boron isotopes (Demicco and others, 2003) by ca. 100 ppm. As expected, good agreement exists between CO_2 estimates from the different stomatal studies with the high, well constrained SI values for *Ginkgo,* but with our estimates from *Metasequoia* leaves giving CO_2 values c. 10 percent higher.

Comparison with Inferred Continuous Cenozoic CO_2 History

A further source of atmospheric CO_2 information for comparison with the revised stomatal-based CO_2 estimates, and other proxies included in the IPCC (2007) report,

TABLE 1

Fossil Ginkgo *(plain font) and* Metasequoia *(italic font) cuticle ages, mean stomatal index (SI), SI standard deviation, previous atmospheric CO_2 reconstructions (Royer and others, 2001b; Retallack, 2002) and our median atmospheric CO_2 reconstructions and their 2.5% and 97.5% quantiles*

Age (Ma)	Mean SI	SI stdev.	Previous CO_2	Median CO_2	2.5% quantile	97.5% quantile
65.5	8.32	1.11	385	538	340	785
64.5	9.48	0.45	339	343	324	673
64.5	9.32	0.77	344	471	327	756
64.1	9.9	0.45	329	331	318	449
64	9.42	0.57	341	367	324	707
61	10.93	0.45	313	317	307	330
58.5	7.55	0.53	450	573	372	791
58.5	7.96	0.45	391	534	364	777
57.3	9.01	0.53	340	447	333	741
56.4	8.75	0.45	348	469	340	738
55.9	10.97	0.45	314	317	306	329
55.9	10.8	0.57	316	319	306	335
55.9	11.43	0.57	311	312	302	325
55.8	10.63	0.69	317	321	305	345
55.7	11.21	0.63	313	315	302	331
55.6	11.5	0.57	311	312	301	325
55.4	12.23	0.53	307	304	296	316
55.3	8.23	0.69	371	520	349	775
55.3	12.18	0.45	308	305	297	314
55.3	11.77	0.77	310	310	296	331
55.3	12.41	0.53	307	303	294	314
55.2	6.54	0.72	798	666	393	803
55.1	8.53	0.94	356	514	342	775
54.8	8.83	0.57	345	479	338	745
53.9	9.29	0.45	334	377	329	713
53.5	10.22	0.6	321	327	312	476
53.4	9.38	0.77	332	443	323	744
16.5	8.14	0.75	377	538	350	781
13.9	14.64	1.43	280	288	252	311
15.7	7.68	0.46	425	554	370	786
15.7	7.86	0.75	425	551	356	788
15.8	7.6	1.3	440	564	350	793
16.5	8.14	0.75	390	533	350	783
15.3	*11.59*	*0.49*	*310*	*313*	*306*	*592*
15.3	*10.94*	*0.63*	*316*	*339*	*309*	*705*
15.2	*10.95*	*0.63*	*316*	*339*	*309*	*705*

is provided by the theoretical approach of Hansen and others (2008) (fig. 4). These authors deconvoluted a Cenozoic global deep ocean and surface air temperature signal from $\delta^{18}O$ measurements on benthic foraminifera shells from ocean sediment cores by accounting for the effect of changes in global ice volume. The resulting ~14 °C Cenozoic temperature change is taken to be forced by changes in atmospheric composition, because other potential climate drivers, including palaeography and solar constant, are either insufficient or of the wrong sign to explain the trends. Assuming approximately 75 percent of the entire Cenozoic climate forcing history by greenhouse gases is contributed by CO_2, and specifying a value of 450 ppm CO_2 at 35

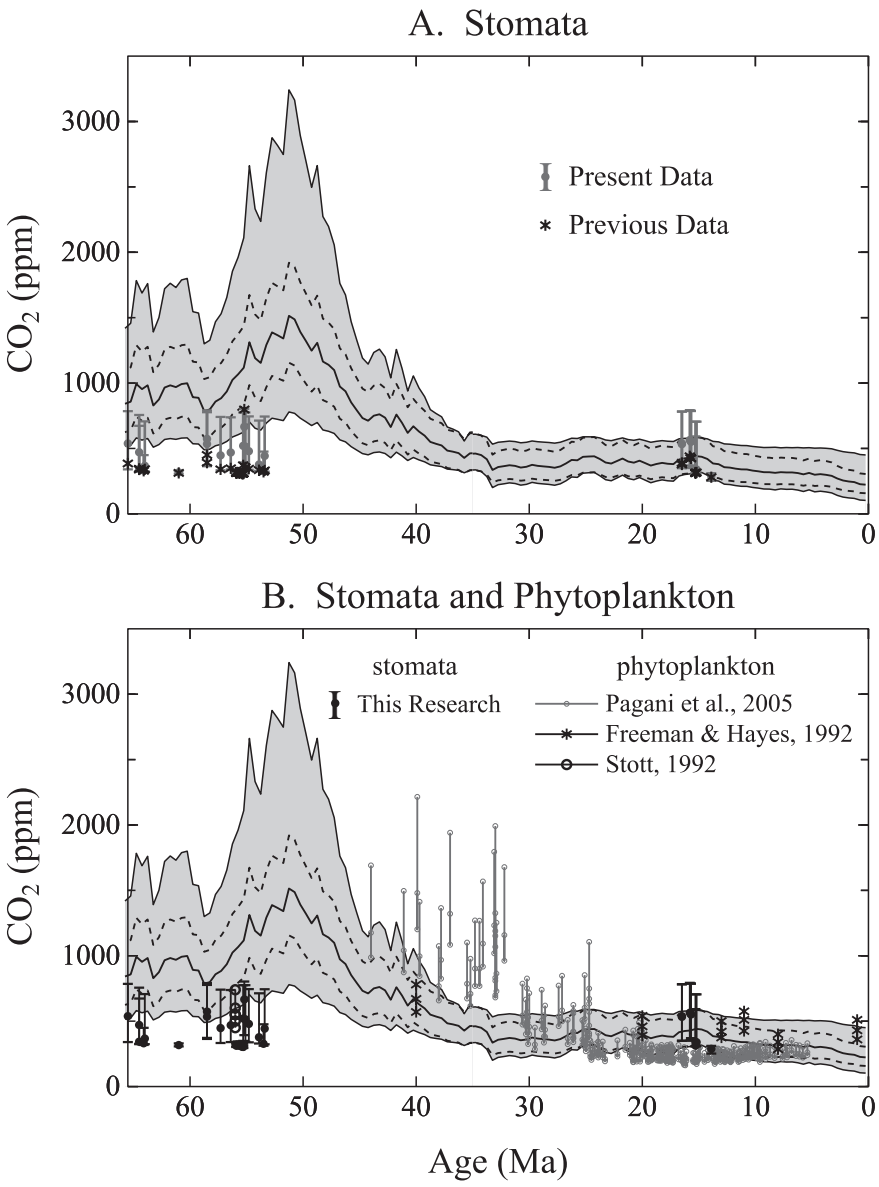

Fig. 4. Continuous Cenozoic atmospheric CO_2 reconstructed compared with (A) CO_2 data indicated by fossil stomata (from fig. 3) and (B) CO_2 data from the alkenone approach. Modeled CO_2 curves in (A) and (B) from Hansen and others (2008). Shaded area delineated by broken lines indicates the effect of changing the anchor CO_2 value at 35 Myr, on which the reconstruction depends, from 450 ppm to either 325 ppm (lower dashed line) or 600 ppm (upper dashed line). Additional uncertainty delineated by the outer envelope indicates the effect of 50% uncertainty in the conversion of change in global ocean temperature to change in global air temperature (Hansen and others, 2008).

Ma, allows the implied changes in CO_2 over the past 65 Myr to be estimated (fig. 4). The reconstruction is anchored 35 Ma, which marks Earth's transition from a largely unglaciated to a glaciated state, for several reasons. Critically, it reproduces the amplitude and mean ice core records of CO_2 spanning the last four glacial cycles of the

Pleistocene (Hansen and others, 2008), and is in general agreement with the CO_2 threshold for Antarctica glaciation determined from climate modeling studies (DeConto and Pollard, 2003).

Figure 4A indicates the higher revised stomatal CO_2 estimates, with the error terms calculated here, begin to consistently overlap the lower bound of the Hansen and others (2008) CO_2 reconstruction in the Paleogene and Neogene. Uncertainties in the reconstruction, depicted by the shaded area of the curve, are associated with the conversion of deep ocean temperature change to surface air temperature change, which differs between ice-free and glaciated worlds, and variations from the standard case of 450 ppm at 35 Ma (Hansen and others, 2008). Alkenones from phytoplankton provide the most temporally detailed CO_2 proxy for the Cenozoic and, when combined with the stomatal CO_2 records, a more coherent pattern of CO_2 change from the proxies for the past 65 Myr begins to emerge (fig. 4B). Few CO_2 estimates between the two proxies overlap, and a priority requirement for future studies should be a cross-validation for different materials of similar ages.

Climate Change and Climate Sensitivity

To a first approximation, revised atmospheric CO_2 concentrations can be translated into global mean surface temperature change (ΔT, GMST) relative to the pre-industrial value using a simple greenhouse formulation that accounts for changes in the solar output over geologic time (Berner, 2004), as given by

$$\Delta T = \Gamma \ln RCO_2 - W_s(t/570) \quad (3)$$

where Γ is a coefficient derived from general circulation modeling, RCO_2 is ratio of mass of CO_2 in the atmosphere at time t to that of the pre-industrial value (280 ppm) and W_s expresses the effect on temperature of the linear increase in solar radiation with time (7.4).

To facilitate a direct comparison of temperature changes resulting from the revised CO_2 estimates with those reported by Royer and others (2001b), we adopted a Γ value of 4.3 in (3). A Γ value of 4.3 corresponds to a rather low climate sensitivity of 2.2 °C to a doubling of CO_2 (that is, $RCO_2 = 2$), calculated as $\ln(RCO_2)4.3 = 2.2$. Accordingly, CO_2-forcing raises global temperatures during the Paleocene and early Eocene by between 1.0 °C and 2.5 °C over previous analyses (fig. 5A). Neogene *Metasequoia* leaf CO_2 estimates gave warmer GMST than before (fig. 5B) by 0.5 to 1.0 °C (Royer and others, 2001b; Retallack, 2002; Royer, 2003). The non-linear nature of the CO_2-temperature relationship magnifies the confidence intervals, some of which span over 3.0 °C (figs. 5A, B). For well constrained CO_2 estimates, calculated ΔTs are typically ca. 0.4 °C below pre-industrial GMST during the middle Paleocene and slightly warmer during the early Eocene. Nevertheless, overall, our revised pattern of ΔT suggests significant CO_2-related greenhouse warming that went unrecognized in earlier studies.

However, an important implication of the stomatal CO_2 reconstructions showing values around 500 to 800 ppm 50 to 65 Myr ago, when the Earth was largely unglaciated, is an implied high climate sensitivity (fig. 3A; fig. 4), defined as the equilibrium sensitivity of the Earth system to a doubling in atmospheric CO_2 (that is inclusion of long-term and short-term feedbacks) (Hansen and others, 2008). A high climate sensitivity appears to be a consistent emerging feature of both empirical and quantitative Cenozoic and Phanerozoic paleoclimate studies, granted limitations in our knowledge of the CO_2 changes involved (table 2).

If Earth's climate sensitivity is higher than 2.2 °C, as seems likely (table 2), then higher values of Γ in equation (1) are more appropriate for computing the change in GMST. Figures 5C and 5D illustrate the effects of an increasing climate sensitivity

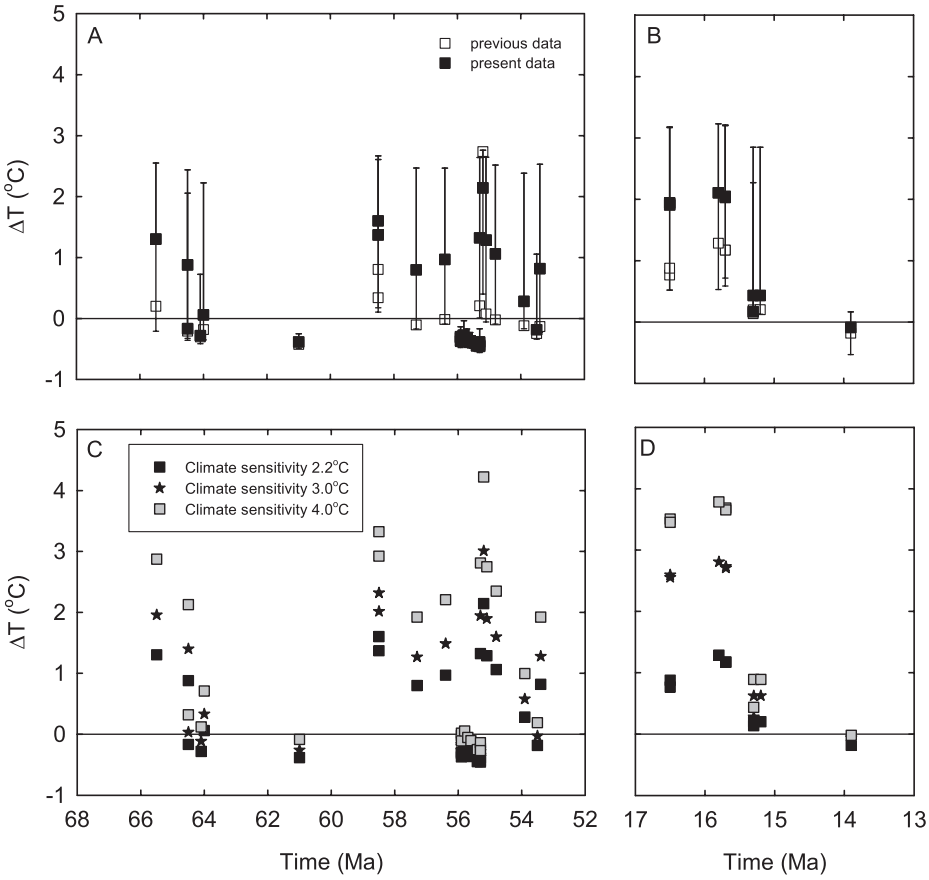

Fig. 5. Calculated changes in global mean surface temperature during the Paleogene (A, C) and Neogene (B, D) based on the CO_2 data given in figure 3. Global mean surface temperature change relative to the pre-industrial due to CO_2 forcing estimated using a simple greenhouse formulation that also accounts for increased solar radiation reaching the Earth's surface over geologic time (see equation 1). The "present data" in A and C display median values ± 95% confidence. Values in panels C and D represent the effect of increasing climate sensitivity to a doubling in CO_2 on the resulting temperature change.

from 2.3 °C to 3.0 and 4.0 °C, calculated with Γ equal to 4.3 and 5.7, respectively, on the predicted ΔT in GMST. The results (figs. 5C, 5D) suggest that global warmth of up 2 to 3 °C above the pre-industrial value could be explained by our revised atmospheric CO_2 estimates and better accord the predominant warm climate regime of the Paleogene and Neogene inferred from independent paleoclimate evidence (Royer, 2006).

CONCLUSION

Improving the utility of fossil leaves when used as biosensors of Earth's ancient atmospheric CO_2 concentration, and indeed other methods of predicting past CO_2, requires assigning realistic uncertainties to the procedures adopted to calibrate and process the fossil data. Critically, the upper boundaries of CO_2 reconstructions from fossil cuticles are likely to be dependent on set data points in the training set at elevated atmospheric CO_2. In some studies, the SI values of fossil cuticles lie outside the training datasets generated either by experiments or from measurements on dated sequences

TABLE 2

Climate sensitivity inferred from paleoclimate studies. [Updated from Hansen and others (2008).]

Interval Studied	Doubled CO_2 sensitivity	Reference
Phanerozoic (0-420 Myr)	~2.8 ºC	Royer and others (2007)
PETM (55.5 Myr)	~4 ºC	Higgins and Schrag (2006)
PETM (55.5 Myr)	High	Pagani and others (2006)
PETM (55.5 Myr)	High	Zeebe and others (2009)
Cenozoic (0-65 Myr)	~ 6.0 ºC	Hansen and others (2008)
Cenozoic (15-65.5 Myr)	High	This study

of herbarium leaves responding to the pre-industrial-to-present CO_2 increase of 280 to 380 ppm (for example, Kürschner and others, 1997, 2008; Retallack, 2001, 2002). Ancient atmospheric CO_2 levels obtained by extrapolating beyond the range of existing training sets are likely to undermine the utility of this paleobiological proxy. Where this situation arises, additional atmospheric CO_2 enrichment experiments with appropriate plant species are called for. These will permit the generation of calibration functions across a broader range of CO_2 levels to provide firmer constrains on high CO_2 estimates from fossil leaf SI inversions. Nevertheless, a significant issue with the technique remains concerning whether the phenotypic responses of plants (that is, limited changes usually within a single generation) revealed by such short-term CO_2 enrichment experiments adequately captures the longer-term (presumably genotypic) response represented by fossils (Beerling and Chaloner, 1993).

ACKNOWLEDGMENTS

We thank Makiko Sato (NASA/Goddard Institute for Space Studies) for kindly drafting figure 4, Dana Royer for information and details on the stomatal indices calibration datasets, and Mark Pagani, Robert Berner and Dana Royer for helpful comments on the manuscript. DJB gratefully acknowledges funding of this work through a Leverhulme Trust award and a Royal Society-Wolfson Research Merit Award.

REFERENCES

Beerling, D. J., and Chaloner, W. G., 1993, Evolutionary responses of stomatal density to global CO_2 change: Biological Journal of the Linnean Society, v. 48, p. 343–353, doi:10.1016/0024-4066(93)90005-9.

Beerling, D. J., and Osborne, C. P., 2002, Physiological ecology of Mesozoic polar forests in a high CO_2 environment: Annals of Botany, v. 89, p. 1–11, doi:10.1093/aob/mcf045.

Beerling, D. J., and Royer, D. L., 2002a, Reading a CO_2 signal from fossil stomata: New Phytologist, v. 153, p. 387–397, doi:10.1046/j.0028-646X.2001.00335.x.

——— 2002b, Fossil plants as indicators of the Phanerozoic global carbon cycle: Annual Review of Earth and Planetary Science, v. 30, p. 527–556, doi:10.1146/annurev.earth.30.091201.141413.

Bergmann, D. C., Lukowitz, W., and Somerville, C. R., 2004, Stomatal development and pattern controlled by a MAPKK kinase: Science, v. 304, p. 1494–1497, doi:10.1126/science.1096014.

Berner, R. A., 2004, The Phanerozoic Carbon Cycle: CO_2 and O_2: Oxford, Oxford University Press, 158 p.

Breecker, D. O., Sharp, Z. D., and McFadden, L. D., 2009, Seasonal bias in the formation and stable isotopic composition of pedogenic carbonate in modern soils from Central New Mexico, USA: Geological Society of America Bulletin, v. 121, p. 630–640.

DeConto, R. M., and Pollard, D., 2003, Rapid Cenozoic glaciation of Antarctica induced by declining atmospheric CO_2: Nature, v. 421, p. 245–249, doi:10.1038/nature01290, doi:10.1038/nature01290.

Demicco, R. V., Lowenstein, T. K., and Hardie, L. A., 2003, Atmospheric pCO_2 since 60 Ma from records of

seawater pH, calcium, and primary carbonate mineralogy: Geology, v. 31, p. 793–796, doi:10.1130/G19727.1.
Ekart, D. D., Cerling, T. E., Montañez, I. P., and Tabor, N. J., 1999, A 400 million year carbon isotope record of pedogenic carbonates: implications for paleoatmospheric carbon dioxide: American Journal of Science, v. 299, p. 805–827, doi:10.2475/ajs.299.10.805.
Enters, D., Kirchner G., and Zolitschka, B., 2006, Establishing a chronology for lacustrine sediments using a multiple dating approach—a case study from the Frickenhauser See, Central Germany: Quaternary Geochronology, v. 1, p. 249–260, doi:10.1016/j.quageo.2007.01.005.
Fletcher, B. J., Brentnall, S. J., Anderson, C. W., Berner, R. A., and Beerling, D. J., 2008, Atmospheric carbon dioxide linked with Mesozoic and early Cenozoic climate change: Nature Geoscience, v. 1, p. 43–48, doi:10.1038/ngeo.2007.29.
Freeman, K. H., and Hayes, J. M., 1992, Fractionation of carbon isotopes by phytoplankton and estimates of ancient CO_2 levels: Global Biogeochemical Cycles, v. 6, p. 185–198, doi:10.1029/92GB00190.
Freeman, K. H., and Pagani, M., 2005, Alkenone-based estimates of past CO_2 levels: a consideration of their utility based on analyses of their uncertainties, *in* Ehleringer, J. R., Cerling, T. E., and Dearing, D. M., editors, A history of atmospheric CO_2 and its effects on plants, animals, and ecosystems: Berlin, Springer, p. 35–61, doi:10.1007/0-387-27048-5_3.
Gray, J. E., Holroyd, G. H., Van Der Lee, F. M., Bahrami, A. R., Sijmons, P. C., Woodward, F. I., Schuch, W., and Hetherington, A. M., 2000, The *HIC* signalling pathway links CO_2 perception to stomatal development: Nature, v. 408, p. 713–716, doi:10.1038/35047071 Letter.
Hansen, J., Sato, M., Kharecha, P., Beerling, D. J., Berner, R. A., Masson-Delmonte, V., Pagani, M., Raymo, M., Royer, D. L., and Zachos, J. C., 2008, Target atmospheric CO_2: where should humanity aim?: The Open Atmospheric Science Journal, v. 2, p. 217–231, doi:10.2174/1874282300802010217.
Henderiks, J., and Pagani, M., 2007, Refining ancient carbon dioxide estimates: significance of coccolithophore cell size for alkenone-based pCO_2 records: Paleoceanography, v. 22, PA3302, doi:10.1029/2006PA001399.
Higgins, J. A., and Schrag, D. P., 2006, Beyond methane: Towards a theory for Paleocene-Eocene thermal maximum: Earth and Planetary Science Letters, v. 245, p. 523–537, doi:10.1016/j.epsl.2006.03.009.
Intergovernmental Panel on Climate Change (IPCC), 2007, Climate Change 2007, The Physical Science Basis: Cambridge, Cambridge University Press, p. 996.
Konrad, W., Roth-Nebelsick, A., and Grein, M., 2008, Modelling of stomatal density response to atmospheric CO_2: Journal of Theoretical Biology, v. 253, p. 638–658, doi:10.1016/j.jtbi.2008.03.032.
Kürschner, W. M., Wagner, F., Visscher, E. H., and Visscher, H., 1997, Predicting the response of leaf stomatal frequency to a future CO_2-enriched atmosphere: constraints from historical observations: Geolische Rundschau, v. 86, p. 512–517, doi:10.1007/s005310050158.
Kürschner, W. M., Kvacek, Z., and Dilcher, D. L., 2008, The impact of Miocene atmospheric carbon dioxide fluctuations on climate and the evolution of terrestrial ecosystems: Proceedings of the National Academy of Sciences, v. 105, p. 449–453, doi:10.1073/pnas.0708588105.
Lake, J. A., Quick, W. P., Beerling, D. J., and Woodward, F. I., 2001, Plant development—Signals from mature to new leaves: Nature, v. 411, p. 154–154, doi:10.1038/35075660.
McElwain, J. C, 2004, Climate-independent paleoaltimetry using stomatal density in fossil leaves as a proxy for CO_2 partial pressure: Geology, v. 32, p. 1017–1020. doi:10.1130/G20915.1.
Pagani, M., Zachos, J. C., Freeman, K. H., Tipple, B., and Bohaty, S., 2005, Marked decline in atmospheric carbon dioxide concentrations during the Paleogene: Science, v. 309, p. 600–603, doi:10.1126/science.1110063.
Pagani, M., Caldeira, K., Archer, D., and Zachos, J. C., 2006, An ancient carbon mystery: Science, v. 314, p. 1556–1557, doi:10.1126/science.1136110.
Ramsay, J. O., 1998, Estimating smooth monotone functions: Journal of the Royal Statistical Society B, v. 60, p. 365–375, doi:10.1111/1467-9868.00130.
Ramsay, J. O., and Silverman, B. W., 2002, Applied Functional Data Analysis: Methods and Case Studies: Berlin, Springer, 190 p.
Retallack, G. J., 2001, A 300-million-year record of atmospheric carbon dioxide from fossil plant cuticles: Nature, v. 411, p. 287–290, doi:10.1038/35077041.
——— 2002, Carbon dioxide and climate over the past 300 Myr: Philosophical Transactions of the Royal Society, v. A360, p. 659–673, doi:10.1098/rsta.2001.0960.
Royer, D. L., 2003, Estimating latest Cretaceous and Tertiary atmospheric CO_2 from stomatal indices, *in* Wing, S. L., Gingerich, P. D., Schmitz, B., and Thomas, E., editors, Causes and Consequences of Globally Warm Climates in the Early Paleogene: Boulder, Colorado, Geological Society of America Special Paper 369, p. 79–93.
——— 2006, CO_2-forced climate thresholds during the Phanerozoic: Geochimica et Cosmochimica Acta, v. 70, p. 5665–5675, doi:10.1016/j.gca.2005.11.031.
Royer, D. L., Berner, R. A., and Beerling, D. J., 2001a, Phanerozoic atmospheric CO_2 change: evaluating geochemical and palaeobiological approaches: Earth-Science Reviews, v. 54, p. 349–392, doi:10.1016/S0012-8252(00)00042-8.
Royer, D. L., Wing, S. L., Beerling, D. J., Jolley, D. W., Koch, P. L. Hickey, L. J., and Berner, R. A., 2001b, Palaeobotanical evidence for near present-day levels of atmospheric CO_2 during part of the Tertiary: Science, v. 292, p. 2310–2313, doi:10.1126/science.292.5525.2310.
Royer, D. L., Berner, R. A., and Park, J., 2007, Climate sensitivity constrained by CO_2 concentrations over the past 420 million years: Nature, v. 446, p. 530–532, doi:10.1038/nature05699.
Silverman, B. W., 1986, Density Estimation for Statistics and Data Analysis: London, Chapman and Hall, 176 p.

Stott, L. D., 1992, Higher temperatures and lower oceanic pCO_2: a climate enigma at the end of the Paleocene Epoch: Paleoceanography,v. 7, p. 395–404, doi:10.1029/92PA01183.
Van der Burgh, J., Visscher, H., Dilcher, D. L., and Kürschner, W. M., 1993, Paleoatmospheric signatures in Neogene fossil leaves: Science, v. 260, p. 1788–1790, doi:10.1126/science.260.5115.1788.
Wagner, F., Bohncke, S. J. P., Dilcher, D. L., Kürschner, W. M., van Geel, B., and Visscher H., 1999, Century-Scale Shifts in Early Holocene Atmospheric CO_2 Concentration: Science, v. 284, p. 1971–1973, doi:10.1126/science.284.5422.1971.
Wynn, J. G., 2003, Towards a physically based model of CO_2-induced stomatal frequency response: New Phytologist, v. 157, p. 391–398, doi:10.1046/j.1469-8137.2003.00702.x.
Zeebe, R. E., Zachos, J. C., and Dickens, G. R., 2009, Carbon dioxide forcing alone insufficient to explain Palaeocene-Eocene thermal maximum warming: Nature Geoscience, v. 2, p. 576–580, doi:10.1038/ngeo578.